

Widely Varying Olefin Rotation Geometry in Platinum(II)-Olefin Complexes Containing the η^3 -Allyl Ligand. Molecular Structure, Solution Stability, and Molecular Orbital Studies

Kunio Miki,^{1a} Kazuhiko Yamatoya,^{1a} Nobutami Kasai,^{*1a} Hideo Kurosawa,^{*1a} Akira Urabe,^{1a} Mitsuhiro Emoto,^{1a} Kazuyuki Tatsumi,^{1b} and Akira Nakamura^{1b}

Contribution from the Department of Applied Chemistry, Osaka University, Suita 565, Osaka, Japan, and the Department of Macromolecular Science, Osaka University, Toyonaka 560, Osaka, Japan. Received October 5, 1987

Abstract: The molecular structures of six olefin complexes {[Pt(η^3 -CH₂CMeCH₂)(olefin)(PPh₃)]PF₆ (**2**) (olefin = CH₂=CH₂ (**2a**), CH₂=CHPh (**2b**), CH₂=CHC₆H₄Cl-*o* (**2c**); (*E*)-MeCH=CHPh (**2d**), (*E*)-MeCH=CHMe (**2e**), (*Z*)-MeCH=CHMe (**2f**)) were determined by X-ray diffraction. Crystal data: **2a** monoclinic, space group *P2₁/n*, *a* = 9.610 (2) Å, *b* = 10.786 (4) Å, *c* = 24.082 (8) Å, β = 91.77 (3)°, *Z* = 4; **2b** monoclinic, space group *P2₁/n*, *a* = 15.560 (3) Å, *b* = 11.342 (3) Å, *c* = 17.594 (3) Å, β = 110.91 (3)°, *Z* = 4; **2c** $1/2$ CH₂Cl₂ orthorhombic, space group *Pccn*, *a* = 11.421 (2) Å, *b* = 27.127 (6) Å, *c* = 20.414 (4) Å, *Z* = 8; **2d**-C₆H₆ monoclinic, space group *P2₁/c*, *a* = 11.408 (2) Å, *b* = 14.910 (10) Å, *c* = 21.397 (3) Å, β = 103.17 (2)°, *Z* = 4; **2e** monoclinic, space group *P2₁/c*, *a* = 13.886 (2) Å, *b* = 11.872 (4) Å, *c* = 16.740 (2) Å, β = 91.17 (1)°, *Z* = 4; **2f** monoclinic, space group *P2₁/c*, *a* = 11.149 (2) Å, *b* = 15.460 (3) Å, *c* = 15.701 (2) Å, β = 90.21 (2)°, *Z* = 4. The ethylene ligand in **2a** lies almost in the coordination plane, defined by Pt, P, and the center of gravity of the allyl triangle, with the C=C axis making an angle of 6.0° with this plane (in-plane geometry). Depending on the steric requirement of the olefin substituents, the angle between the C=C axis and the coordination plane varies quite widely (**2b** 11.1°, **2c** 24.5°, **2d** 46.1°, **2e** 67.0°, **2f** 7.4°). The *o*-chloro- and *o*-methyl-substituted styrene complexes of **2** showed considerably smaller solution stabilities than the corresponding meta- and para-substituted counterparts owing to the steric repulsion nearly on the coordination plane between the ortho substituent and the allyl hydrogen, while the reversed stability order was observed in those complexes that contain the C=C axis perpendicular to the coordination plane (upright geometry). The complexes **2** containing (*E*)-olefin ligands showed unprecedented higher stabilities than the corresponding (*Z*)-olefin complexes by a factor of ca. 2. Extended Hückel MO calculations were carried out on [Pt(η^3 -CH₂CHCH₂)(CH₂=CH₂)(PH₃)]⁺ in both in-plane and upright geometries to give comparable total energies for the two conformers. The nature of the Pt-olefin bond in **2** is discussed in terms of these structural and MO results.

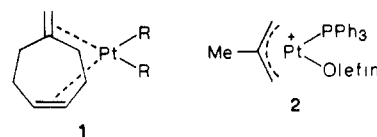
Configuration and bonding of a transition-metal-coordinated olefin ligand are critically affected by electronic and steric characteristics created by the surrounding ligand framework.² Three classes of platinum-olefin complexes well illustrate such a view. Thus, three-coordinated Pt(0) complexes contain the C=C bond lying parallel with the coordination plane (in-plane geometry hereafter) owing to the enhanced π interaction in this geometry compared to one with the C=C bond perpendicular to the plane (upright geometry).^{2d,e} A somewhat similar reasoning is applied in explaining the C=C bond lying in the trigonal plane of a trigonal bipyramid for five-coordinated Pt(II) complexes.^{2f}

On the other hand, in four-coordinated Pt(II)-olefin complexes, e.g., Zeise's salt and its analogues, the molecular orbital calculations suggested^{2d,e} that the observed upright geometry has resulted from much smaller steric congestion around ethylene in this geometry than in the in-plane geometry. In terms of the electronic factor, there would have been little difference of the π bonding energy between the two geometries.

All the structure determinations of the square-planar olefin complexes had shown the upright geometry³ until Hoffmann and co-workers proposed^{2d} several strategies to stable olefin complexes having the in-plane geometry. Then X-ray structure determination of PtCl₂(5-methylenecycloheptene) (**1**; R = Cl) revealed^{4a} the

first in-plane C=C coordination; in **1** (R = Cl, Ph) as well as their 5-methylenecyclooctene analogues^{4b} the chelate bond formation compelled the exocyclic C=C bond to lie in the desired direction. Subsequently we found the in-plane coordination of simple monoolefin in an apparently four-coordinated Pt(II) complex of the type **2**.⁵

We thought further structure and stability studies of complexes containing the η^3 -allyl and η^2 -olefin ligands simultaneously were very intriguing for several reasons. First, these studies may shed more light on the origin of the in-plane C=C bond geometry found in **2b**. Although the solution chemistry of **2** is known to apparently resemble that of the Zeise's salt class complexes,⁶ it remains to



2: olefin = (a) CH₂=CH₂; (b) CH₂=CHC₆H₅; (c) CH₂=CHC₆H₄Cl-*o*; (d) (*E*)-MeCH=CHC₆H₅; (e) (*E*)-MeCH=CHMe; (f) (*Z*)-MeCH=CHMe

be clarified to what extent the structure of **2b** is related to the electronic requirement for the in-plane geometry in three-coordinated Pt(0) complexes. Or the problem might simply be steric in origin, for the η^3 -allyl ligand exerts a sterically favorable coordination environment on the in-plane olefin by virtue of its small bite angle for a chelate. The nature of the η^3 -allyl-metal bond,

(1) (a) Department of Applied Chemistry. (b) Department of Macromolecular Science.

(2) (a) Collmann, J. P.; Hegedus, L. S. *Principles and Applications of Organotransition Metal Chemistry*; University Science Books: Mill Valley, CA, 1980; p 105. (b) Herberhold, M. *Metal π -Complexes*; Elsevier: Amsterdam, 1974; Vol. 2, Part 2. (c) Hartley, F. R. *Comprehensive Organometallic Chemistry*; Wilkinson, G., Stone, F. G. A., Abel, E. W., Eds.; Pergamon: Oxford, 1982; Vol. 6, Chapter 39. (d) Albright, T. A.; Hoffmann, R.; Thibault, J. C.; Thorn, D. L. *J. Am. Chem. Soc.* **1979**, *101*, 3801 and references therein. (e) Ziegler, T.; Rauk, A. *Inorg. Chem.* **1979**, *18*, 1558. (f) Hartley, F. R. *J. Organomet. Chem.* **1981**, *216*, 277.

(3) Ittel, S. D.; Ibers, J. A. *Adv. Organomet. Chem.* **1976**, *14*, 33.

(4) (a) Wright, L. L.; Wing, R. M.; Rettig, M. F.; Wiger, G. R. *J. Am. Chem. Soc.* **1980**, *102*, 5949. (b) Rakowsky, M. H.; Woolcock, J. C.; Wright, L. L.; Green, D. B.; Rettig, M. F.; Wing, R. M. *Organometallics* **1987**, *6*, 1211.

(5) Miki, K.; Kai, Y.; Kasai, N.; Kurosawa, H. *J. Am. Chem. Soc.* **1983**, *105*, 2482.

(6) Kurosawa, H.; Asada, N. *J. Organomet. Chem.* **1981**, *217*, 259.

Table I. Selected Bond Lengths (Å) with Their Estimated Standard Deviations in Parentheses

	2a	2b	2c	2d	2e	2f
Pt-P(1)	2.306 (4)	2.309 (3)	2.307 (4)	2.295 (2)	2.293 (2)	2.309 (3)
Pt-C(2)	2.224 (17)	2.189 (10)	2.181 (19)	2.218 (8)	2.235 (15)	2.185 (16)
Pt-C(3)	2.253 (16)	2.291 (10)	2.221 (18)	2.269 (8)	2.229 (17)	2.256 (18)
Pt-CET	2.137	2.140	2.096	2.138	2.137	2.119
Pt-C(11)	2.118 (20)	2.156 (11)	2.130 (19)	2.137 (10)	2.144 (12)	2.120 (15)
Pt-C(12)	2.187 (14)	2.199 (11)	2.176 (17)	2.185 (10)	2.182 (14)	2.156 (15)
Pt-C(13)	2.239 (18)	2.210 (11)	2.234 (17)	2.218 (10)	2.244 (12)	2.184 (18)
Pt-CAL	1.927	1.935	1.913	1.918	1.923	1.909
C(1)-C(2)				1.52 (2)	1.46 (3)	1.51 (3)
C(2)-C(3)	1.33 (3)	1.33 (2)	1.36 (3)	1.36 (2)	1.29 (3)	1.33 (3)
C(3)-C(4)		1.49 (2)	1.45 (3)	1.49 (2)	1.44 (3)	1.52 (3)
C(4)-C(5)		1.38 (2)	1.42 (3)	1.38 (2)		
C(5)-C(6)		1.36 (2)	1.30 (4)	1.38 (2)		
C(6)-C(7)		1.43 (2)	1.47 (4)	1.37 (2)		
C(7)-C(8)		1.33 (2)	1.35 (4)	1.39 (2)		
C(8)-C(9)		1.40 (2)	1.38 (3)	1.37 (2)		
C(9)-C(4)		1.39 (2)	1.40 (3)	1.39 (2)		
C(9)-Cl			1.745 (19)			
C(11)-C(12)	1.38 (3)	1.42 (2)	1.39 (3)	1.41 (2)	1.43 (2)	1.38 (3)
C(12)-C(13)	1.41 (3)	1.36 (2)	1.43 (3)	1.39 (2)	1.41 (2)	1.33 (3)
C(12)-C(14)	1.49 (3)	1.47 (2)	1.51 (3)	1.54 (2)	1.55 (3)	1.54 (3)

Table II. Selected Bond Angles (deg) with Their Estimated Standard Deviations in Parentheses

	2a	2b	2c	2d	2e	2f
P(1)-Pt-CET	101.2	105.7	105.4	104.4	102.7	105.3
P(1)-Pt-CAL	130.0	126.1	126.0	124.4	128.1	123.9
CET-Pt-CAL	128.8	127.9	128.3	131.0	128.9	130.7
C(2)-Pt-C(3)	34.6 (6)	34.3 (4)	36.1 (7)	35.3 (3)	33.6 (6)	34.8 (6)
C(1)-C(2)-C(3)				122.5 (8)	131.9 (15)	123.6 (16)
C(2)-C(3)-C(4)		126.8 (10)	127.1 (17)	123.6 (8)	132.8 (16)	124.4 (17)
C(3)-C(4)-C(5)		123.4 (10)	121.5 (15)	123.6 (8)		
C(3)-C(4)-C(9)		117.6 (9)	124.7 (15)	117.2 (8)		
C(5)-C(4)-C(9)		119.0 (10)	113.4 (15)	119.2 (9)		
C(4)-C(5)-C(6)		121.0 (11)	125.6 (20)	120.2 (9)		
C(5)-C(6)-C(7)		120.4 (12)	118.0 (22)	121.1 (10)		
C(6)-C(7)-C(8)		117.4 (12)	119.3 (22)	118.5 (11)		
C(7)-C(8)-C(9)		123.4 (12)	119.5 (20)	121.0 (11)		
C(8)-C(9)-C(4)		118.7 (10)	124.1 (17)	119.8 (10)		
C(4)-C(9)-Cl			118.6 (13)			
C(8)-C(9)-Cl			117.3 (15)			
C(11)-C(12)-C(13)	115.2 (15)	116.2 (10)	118.1 (16)	117.6 (9)	116.6 (12)	116.6 (15)
C(11)-C(12)-C(14)	123.0 (16)	120.1 (10)	122.0 (16)	120.0 (9)	122.7 (12)	122.0 (15)
C(13)-C(12)-C(14)	121.0 (15)	121.7 (10)	118.7 (15)	121.3 (9)	119.4 (12)	120.7 (15)

a clue to the above problem, is not well understood at present, and we hope to gain more insight into this bonding through these studies.

Second, (η^3 -allyl)(η^2 -olefin)metal complexes were shown to play a key role in certain catalytic as well as stoichiometric organic transformations.⁷

We now describe more extensive X-ray structure determinations of olefin complexes **2a-f** which reveal novel variation of the olefin coordination geometry (ranging from in-plane to near upright C=C bond orientation) depending on the steric demand of the olefinic ligand.⁸ We also describe some unusual solution stability trends of **2** which originate from such unique structural aspects. Then we discuss the nature of the Pt-olefin bond in **2** on the basis of the structures determined and the results of the extended Hückel MO calculations.

(7) (a) Keim, W.; Behr, A.; Roper, M., ref 1c, Vol. 8, Chapter 52. (b) Hosokawa, T.; Uno, T.; Inui, S.; Murahashi, S. *J. Am. Chem. Soc.* **1981**, *103*, 2318. (c) Kurosawa, H.; Emoto, M.; Urabe, A.; Miki, K.; Kasai, N. *Ibid.* **1985**, *107*, 8253. (d) Kurosawa, H.; Emoto, M.; Ohnishi, H.; Miki, K.; Kasai, N.; Tatsumi, K.; Nakamura, A. *Ibid.* **1987**, *109*, 6333. (e) Golaszewski, A.; Schwartz, J. *Tetrahedron* **1985**, *41*, 5779 and references therein.

(8) (a) Portions of this work were reported in preliminary forms; see ref 5 and: Miki, K.; Yamatoya, K.; Kasai, N.; Kurosawa, H.; Emoto, M.; Urabe, A. *J. Chem. Soc., Chem. Commun.* **1984**, 1520. (b) A recent report described another example of nearly in-plane coordination of the C=C bond to the η^3 -allyl-bound Pd atom where the olefinic moiety is part of the η^3 -allyl substituent: Ciajolo, R.; Jama, M. A.; Tuzi, A.; Vitagliano, A. *J. Organomet. Chem.* **1985**, *295*, 233.

(9) Johnson, C. K. ORTEP-II, Report ORNL-5138, Oak Ridge National Laboratory, Tennessee, 1976.

Results and Discussion

Crystal Structure Elucidation of Various Olefin Coordination Geometry. Figure 1 represents the molecular structure of **2a** as projected onto the coordination plane, defined by Pt and P atoms and the center of gravity of the allyl triangle (CAL). Figure 2 shows the perspective drawings of [Pt(η^3 -CH₂CMeCH₂)(olefin)(PPh₃)] cations for **2a-f** as viewed from the midpoint of the olefinic C=C bond (CET) to the Pt atom. Selected bond lengths and angles are listed in Tables I and II. Full listings of the tables for bond lengths and angles and the equations of least-square planes are available as supplementary material (Tables S2-S4).

In all the structures determined, the Pt and P atoms, CAL, and CET are coplanar with each other, the maximum atomic deviation from the least-squares plane being 0.015, 0.054, 0.044, 0.042, 0.045, and 0.030 Å for **2a-f**, respectively. The geometrical arrangement of the P atom, CAL, and CET around the Pt atom is similar to each other except for small but significant changes in the bond angles (see later). The conformation of three phenyl rings of PPh₃ about the Pt-P axis is different in **2a** from those in the others.

The most remarkable and interesting feature of the molecular structures of **2a-f** is widely varying olefin coordination geometry, no precedent of which has yet been reported in four-coordinated Pt(II) and three-coordinated Pt(0)-olefin complexes. Thus, the angle between the olefinic C=C bond and the coordination plane was found to be 6.0°, 11.1°, 24.5°, 46.1°, 67.0°, and 7.4° for **2a-f**, respectively. By way of contrast, the known rotation angle of the coordinated *E*-olefin, which usually shows the largest distortion,

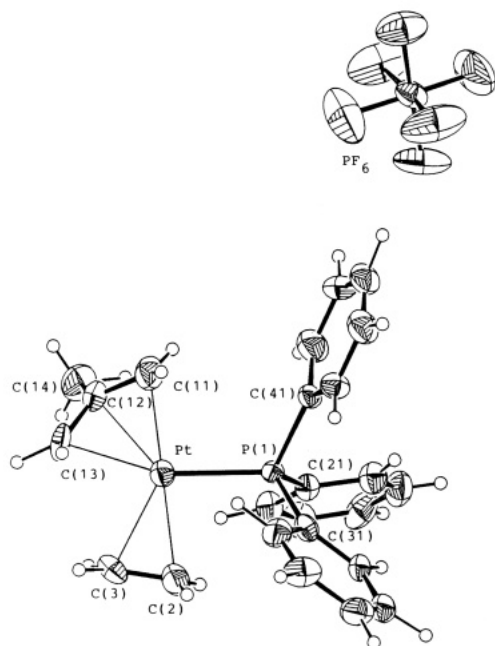


Figure 1. The molecular structure of **2a** as projected onto the coordination plane of platinum (ORTEP drawing⁹) along with selected atomic numberings. Non-hydrogen atoms are represented by thermal ellipsoids at 30% probability levels, whereas hydrogen atoms are drawn by the sphere with $B = 1.0 \text{ \AA}^2$.

from the most stable C=C orientation in the parent ethylene complex is in the range 9–17° for the Pt(II)¹⁰ and 5–9° for the Pt(0)¹¹ complexes.

No abnormally short intermolecular atomic contacts, which are less than the sum of the van der Waals radii of the two atoms, are observed in either complex. This suggests that the crystal packing force does not play any dominant role in determining the geometry of the C=C bond. The observed geometries are most probably a function of both electronic and steric factors, the latter being of intramolecular nature, as discussed below.

Molecular models¹² indicated that rotation of ethylene, both clockwise and anti-clockwise, from its position found in **2a** up to the upright one brings about the slightly larger steric congestion at the early stages, but rather the smaller congestion is attained at the 90° rotation. This may lead us to assume an electronic force to keep ethylene in-plane coordinated. The same force may also apply in the styrene complex **2b**. In the case of *o*-chloro-substituted styrene, however, adoption of the same geometry as that in **2b** would have generated some repulsion between Cl and the *syn*-hydrogen atom attached to C(13); the Cl...H contact in **2c** set in a hypothetical, near in-plane geometry was calculated as 2.86 Å. Occurrence of the larger rotation in **2c** than **2b** suggests that the electronic force to keep the C=C bond in-plane coordinated is not large enough to compensate the Cl...H repulsion.

Putting the methyl substituent at the β position of the in-plane coordinated styrene no doubt results in very severe repulsion with the phosphine ligand, forcing the olefin in **2d** to rotate to such a position as was observed. A further rotation would have relieved the congestion about the methyl substituent still more. We assume

(10) (a) Benedetti, E.; Corradini, P.; Pedone, C. *J. Organomet. Chem.* **1969**, *18*, 203. (b) Spagna, R.; Venanzi, L. M.; Zambonelli, L. *Inorg. Chim. Acta* **1970**, *4*, 283. (c) Spagna, R.; Zambonelli, L. *J. Chem. Soc. A* **1971**, 2544. (d) Spagna, R.; Ughetto, G.; Zambonelli, L. *Acta Crystallogr. B* **1973**, *29*, 1151.

(11) (a) Panattoni, C.; Graziani, R.; Bandoli, G.; Clemente, D. A. *J. Chem. Soc. B* **1970**, 371. (b) Baraban, J. M.; McGinnety, J. A. *Inorg. Chem.* **1974**, *13*, 2864.

(12) These also incorporate the Lennard-Jones type potential calculations, $U = \sum[(d_{ij}/r_{ij}^{12}) - (e_{ij}/r_{ij}^6)]$ where r_{ij} is the distance between the *i*th atom in olefin and the *i*th atom in the ligands of Pt(η^3 -CH₂CMeCH₂)(PPh₃), and d_{ij} and e_{ij} are constants which depend on the atom types for repulsive and attractive terms, respectively; Scott, R. A.; Scheraga, H. A. *J. Chem. Phys.* **1966**, *45*, 2091.

Table III. Stability Constants^a of Substituted Styrene Complexes

X	M =	M =	M =
	[Pt(η^3 -C ₄ H ₇)(PPh ₃) ⁺] 2	<i>trans</i> -PtCl ₂ (py) 3	[Pd(η^5 -C ₅ H ₅)(PPh ₃) ⁺] 4
<i>o</i> -Me	0.34 ± 0.08	3.1 ± 0.3 ^b	2.1 ± 0.5
<i>m</i> -Me	1.4 ± 0.3	1.3 ± 0.2	1.4 ± 0.2 ^c
<i>p</i> -Me	1.6 ± 0.3 ^d	1.8 ± 0.4 ^b	1.7 ± 0.2 ^c
<i>o</i> -Cl	0.27 ± 0.02	0.72 ± 0.09 ^b	1.4 ± 0.3
<i>m</i> -Cl	0.40 ± 0.04	0.72 ± 0.09	0.26 ± 0.04 ^c
<i>p</i> -Cl	0.49 ± 0.10 ^d	0.78 ± 0.09 ^b	0.56 ± 0.06 ^c

^a K_1 values of eq 1 in CDCl₃ at 25 °C (2), -25 °C (3) or -2 °C (4).

^b Reference 19. ^c Reference 17a. ^d Reference 6.

that this excessive rotation was not realized, for the phenyl substituent would have suffered from new congestion with the phosphine through such rotation. This assumption was confirmed by the still larger degree of rotation in **2e** where the phenyl substituent of (*E*)- β -methylstyrene is replaced by the smaller methyl group.

The intermediate degree of rotation cannot relieve the congestion about the Z-olefins. Molecular models¹² suggested that along the rotation of (*Z*)-2-butene about the Pt-olefin axis, there exist three minima in terms of the steric repulsion energy (two in-plane and one upright geometries); the steric congestion is about the same in the two in-plane geometries and one of the upright geometries with two methyls directed to the allylic ligand side. The electronic factor has most probably dominated in determining the observed coordination geometry of **2f**. The in-plane accommodation of the sterically much demanding (*Z*)-2-butene by the Pt(η^3 -methallyl)(PPh₃) moiety is noteworthy, even though the P-Pt-CAL angle is a little narrowed compared to those of the other complexes except for **2d** (see Table II).

Of the symmetrically substituted olefin complexes, the two Pt-C(olefin) lengths are similar in **2e** but differ considerably in the in-plane complexes **2a** and **2f**. In these complexes the Pt-C(3) bond, which is *transoid* to the P atom, is longer than the *cisoid* Pt-C(2) bond, a trend that is quite the reverse of those found in Pt(0) complexes of the type Pt(PR₃)(CH₂=CH₂)(olefin) (olefin = duroquinone, CF₂=CF₂).¹³ All the Pt-C(olefin) lengths in the present complexes (2.181–2.291 Å) are somewhat longer than those of the known square-planar Pt(II) complexes containing simple monoolefins (2.10–2.26 Å)^{10,14} except for one containing a strongly electron-releasing substituent ((*Z*)-Me₂CHCH=CHNHC₆H₄Cl; 2.31 Å).^{14t} The C=C bond lengths in **2a–f** are also among the shortest in the known Pt-olefin complexes.

The coordination mode of the allyl group to the metal is asymmetrical. Three Pt-C(allyl) bonds are lengthened in each complex in the order Pt-C(11) < Pt-C(12) < Pt-C(13). This is the same trend as that found in Pd(η^3 -methallyl)(Cl)(PPh₃).¹⁵ The allyl plane defined by C(11), C(12), and C(13) is declined

(13) Chetcuti, M. J.; Herbert, J. A.; Howard, J. A. K.; Pfeffer, M.; Spencer, J. L. *J. Chem. Soc., Dalton Trans.* **1981**, 284.

(14) (a) Spagna, R.; Venanzi, L. M.; Zambonelli, L. *Inorg. Chim. Acta* **1970**, *4*, 475. (b) Colapietro, M.; Zambonelli, L. *Acta Crystallogr. B* **1971**, *27*, 734. (c) Merlino, S.; Lazzaroni, R.; Montagnoli, G. *J. Organomet. Chem.* **1971**, *30*, C93. (d) Spagna, R.; Zambonelli, L. *Acta Crystallogr. B* **1972**, *28*, 2760. (e) Kops, R. T.; van Aken, E.; Scheck, H. *Ibid.* **1973**, *29*, 913. (f) Cotton, F. A.; Francis, J. N.; Frenz, B. A.; Tsutsui, M. *J. Am. Chem. Soc.* **1973**, *95*, 2483. (g) Loves, R. A.; Koetzle, T. F.; Williams, G. J. B.; Andrews, L. C.; Bau, R. *Inorg. Chem.* **1975**, *14*, 2653. (h) Nyburg, S. C.; Simpson, K.; Wong-Ng, W. *J. Chem. Soc., Dalton Trans.* **1976**, 1865. (i) Mura, P.; Spagna, R.; Ughetto, G.; Zambonelli, L. *Acta Crystallogr. B* **1976**, *32*, 1151. (j) Bresciani Pahor, N.; Calligalis, M.; Delise, P.; Randaccio, L.; Maresca, L.; Natile, G. *Inorg. Chim. Acta* **1976**, *19*, 45. (k) Ball, R. G.; Payne, N. C. *Inorg. Chem.* **1976**, *15*, 2494. (l) Ball, R. G.; Payne, N. C. *Ibid.* **1977**, *16*, 45. (m) Mura, P.; Spagna, R.; Zambonelli, L. *Acta Crystallogr. B* **1978**, *34*, 3745. (n) Caruso, F.; Spagna, R.; Zambonelli, L. *J. Cryst. Mol. Struct.* **1978**, *8*, 47. (o) Tiripicchio, A.; Tiripicchio Camellini, M.; Maresca, L.; Natile, G.; Rizzardi, G. *Cryst. Struct. Commun.* **1979**, *8*, 689. (p) Caruso, F.; Spagna, R.; Zambonelli, L. *Inorg. Chim. Acta* **1979**, *32*, L23. (q) Briggs, J. R.; Crocker, C.; McDonald, W. S.; Shaw, B. L. *J. Organomet. Chem.* **1979**, *181*, 213. (r) Briggs, J. R.; Crocker, C.; McDonald, W. S.; Shaw, B. L. *J. Chem. Soc., Dalton Trans.* **1980**, 64. (s) Camalli, M.; Caruso, F.; Zambonelli, L. *Inorg. Chim. Acta* **1980**, *44*, L177. (t) De Renzi, A.; Ganis, P.; Panunzi, A.; Vitagliano, A.; Valle, G. *J. Am. Chem. Soc.* **1980**, *102*, 1722. (u) Johnson, D. A.; Deese, W. C.; Cordes, A. W. *Acta Crystallogr. B* **1981**, *37*, 2220. (15) Mason, R.; Russell, D. R. *J. Chem. Soc., Chem. Commun.* **1966**, 26.

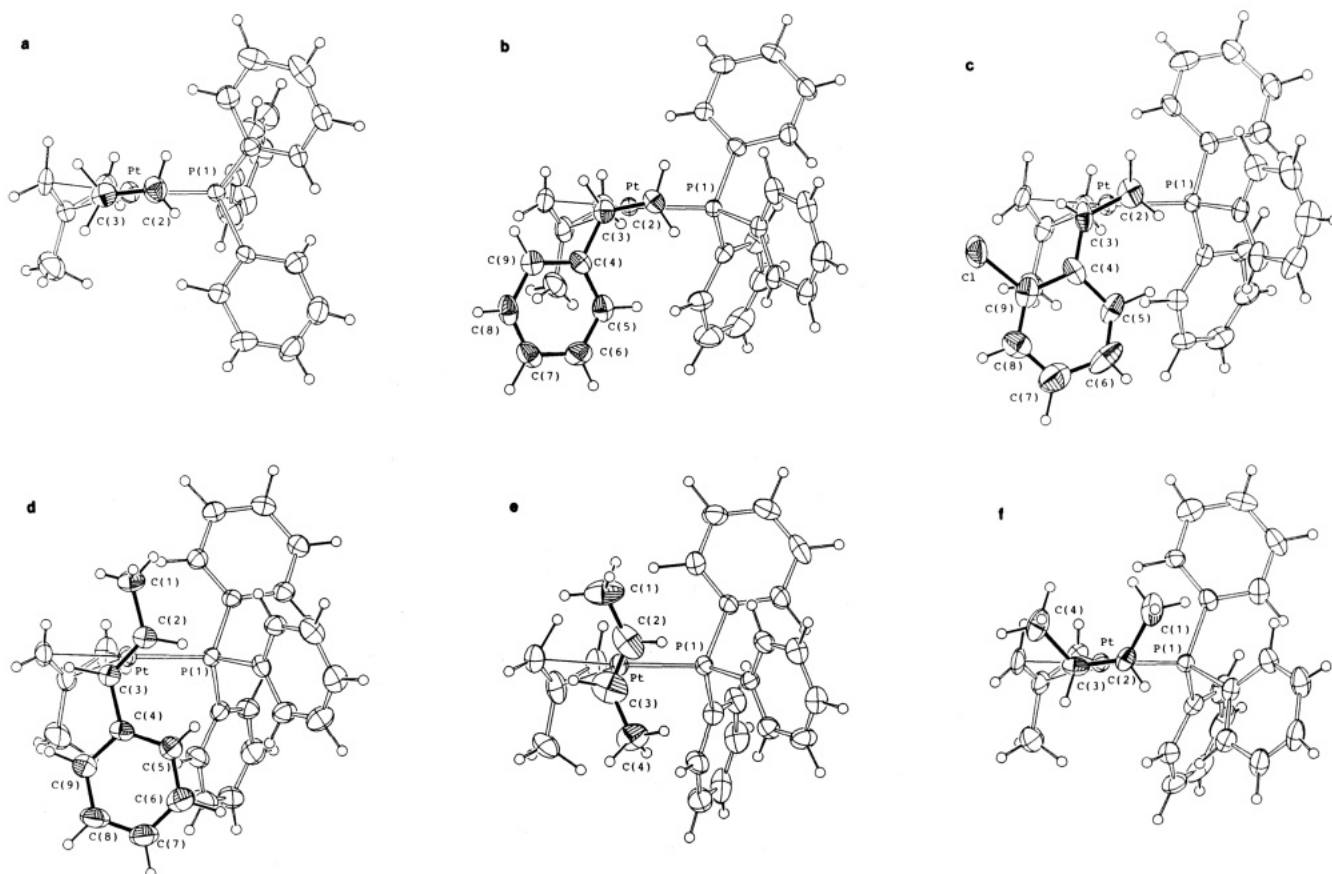


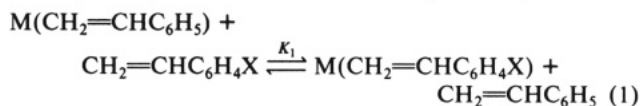
Figure 2. The perspective drawings (ORTEP⁹) of the $[\text{Pt}(\eta^3\text{-CH}_2\text{CMeCH}_2)(\text{PPh}_3)(\text{olefin})]$ cations as viewed from the midpoint of the olefinic C=C bond to the platinum atom along with the atomic numbering scheme of the olefin. Atoms are represented by the same condition as Figure 1. Olefin = $\text{CH}_2=\text{CH}_2$ (a), $\text{CH}_2=\text{CHPh}$ (b), $\text{CH}_2=\text{CHC}_6\text{H}_4\text{Cl-}o$ (c), (*E*)- $\text{MeCH}=\text{CHPh}$ (d), (*E*)- $\text{MeCH}=\text{CHMe}$ (e), (*Z*)- $\text{MeCH}=\text{CHMe}$ (f).

to the coordination plane with the dihedral angles of 115.2°, 116.7°, 116.9°, 117.7°, 115.2°, and 115.6° for **2a–f**, respectively.

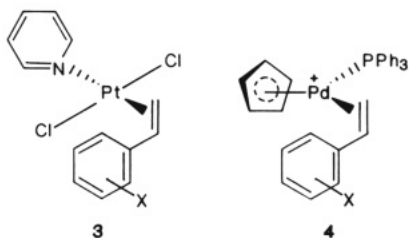
Structures and Stabilities in Solution. It seems of special interest to know how some behaviors of **2** in solutions are related to the solid-state structures so far described. ¹H NMR data¹⁶ of **2b** are consistent with preservation of the in-plane geometry shown in Figure 2b also in solution. However, they may not necessarily be regarded as convincing evidence for the in-plane geometry, particularly in view of the insufficient accumulation of relevant NMR data. Of particular interest in this regard would be to examine the solution stability trends of **2** containing some specifically substituted olefin ligands, since the in-plane C=C coordination such as that in **2a** is expected to receive different steric effects than the upright coordination.

First we point out a unique stability trend of **2** containing ortho-substituted styrenes. Table III summarizes relative stabilities of various substituted styrene complexes of **2**, as expressed by K_1 of eq 1, together with those of **3** and **4** which contain the upright coordinated C=C bond.^{3,17} Notably, introduction of *o*-methyl

and *o*-chloro substituents had a contrasting effect on the stabilities of **2** on one hand and those of **3** and **4** on the other. Thus, the ortho-substituted styrene complexes of **2** are *less stable* than the corresponding para- and meta-substituted styrene complexes,¹⁸ while in **3** and **4** the ortho-substituted styrene complexes give K_1 values *comparable to or greater than* the para- and meta-substituted derivatives. It seems relevant to point out here that both **3** and **4** have the electronic demand on the stability trends similar to that for **2** as suggested by the Hammett equations for the stability of the para- and meta-substituted styrene complexes.^{6,17–19}



The lower stability of the ortho-substituted styrene complexes in **2** can be understood by the repulsion between the substituent and the allylic hydrogen. This may elongate the metal–olefin bond length and/or distort the C=C bond as was found in the solid-state structure of **2c**. The latter distortion may bring about loss of π bond energy to some extent (see later). However, since the degree of the decrease in the stability of **2c** is not so large, the electronic force to keep the C=C bond in the in-plane geometry in **2** would be rather small (see later). In the upright geometry in **3** and **4**, the ortho substituent would experience much smaller steric congestion than in **2**. In such a case, electronic, rather than steric, factors such as the polar effect which is especially prominent in the ortho substituent²⁰ might be more important, even though a



(16) The resonances of H^{tr} and H^{cis} (with respect to the Ph substituent) of styrene, located close to PPh_3 in Figure 2b, received considerable up-field shifts (1.41 and 1.49 ppm) and exhibited ³¹P couplings (3.0 and 7.2 Hz), while that of H^{sm} showed the much smaller up-field shift (0.17 ppm) with no ³¹P coupling.⁶ Similar effects of PPh_3 on nearby olefinic proton resonances were noted in the complexes of type $[\text{M}(\eta^3\text{-C}_3\text{H}_5)(\text{olefin})(\text{PPh}_3)]^+$ (M = Pd, Pt).¹⁷

(17) (a) Kurosawa, H.; Majima, T.; Asada, N. *J. Am. Chem. Soc.* **1980**, *102*, 6996. (b) Miki, K.; Shiotani, O.; Kai, Y.; Kasai, N.; Kanatani, H.; Kurosawa, H. *Organometallics* **1983**, *2*, 585.

(18) Stabilities of meta-substituted styrene complexes of **2** are well within the range of the already established Hammett relationship.⁶

(19) Kurosawa, H.; Urabe, A.; Emoto, M. *J. Chem. Soc., Dalton Trans.* **1986**, 891.

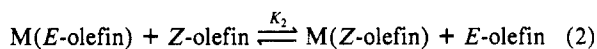
Table IV. Relative Stability of *E*- and *Z*-Olefin Complexes of **2**

olefin	K_2^a
MeCH=CHMe	0.45 ± 0.10
MeCH=CHEt	0.48 ± 0.10
MeCH=CHPh	0.25 ± 0.10

^aEquilibrium constants of eq 2 ($M = [\text{Pt}(\eta^3\text{-CH}_2\text{CMeCH}_2\text{-PPh}_3)]^+$) in CDCl_3 at 25 °C.

more precise mechanism for the increase of the stability by the ortho substitution remains to be elucidated.

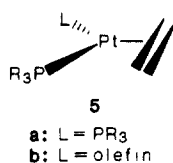
Another unusual stability trend in **2** concerns the relative coordination ability of an *E/Z*-olefin pair. The relative stabilities of pairs of *E/Z*-olefin complexes of **2** were determined by NMR spectroscopy (eq 2), as summarized in Table IV. Of particular note in Table IV is that the K_2 values are smaller than unity, showing the higher stability of the *E*- than the *Z*-olefin complexes. These values may be contrasted to those (>2) for the more regular square-planar complexes of Rh(I), Pd(II), and Pt(II).^{14a,19,21}



We assume that introducing two substituents at 1,2-positions (*E* and *Z* geometry) of ethylene generates very large steric congestion, particularly in the case of the in-plane geometry complex such as **2**. A considerable portion of this congestion would be relieved only for the *E*-olefin complex by rotating the C=C bond, as revealed in Figure 2d,e. Thus, the *E*-olefin complex of **2** may contain considerably less steric congestion than the *Z*-olefin complex. This difference should be compensated by loss of π bonding energy caused by rotation of the C=C bond. However, this π bonding energy loss would not be very large in the complexes of the type **2** (see next section), resulting in the *E*-olefin complex more stable than the *Z*-olefin complex.

The origin of the observed relative stability of *E/Z*-olefin pairs in the more ordinary complexes seems less clear. As described before, the structural studies indicated that the rotational distortion of *E*-olefins from the upright position in the Zeise's salt class of complexes is not so remarkable¹⁰ as those found in **2d** and **2e**. It may well be that the degree of steric congestion generated by 1,2-disubstitution of the upright ethylene ligand is not so severe as that in the in-plane case. Or excessive rotation of the *E*-olefin might have induced an abrupt increase of the repulsion between the olefinic hydrogens and the cis ligand groups. In any case, the difference in the steric congestion around two isomeric olefins would remain relatively small. In such a case, the difference in the internal strain of the free olefin which is relieved upon complexation (*Z*-olefin $>$ *E*-olefin) may be a primary determinant for the relative coordination ability of *E*- and *Z*-olefins.^{2c}

Nature of the Pt-Olefin Bond. It has been well recognized that olefins in $\text{Pt}(\text{olefin})(\text{L})(\text{PR}_3)$ (**5**: L = PR_3 (**a**), olefin (**b**)) prefer the in-plane coordination geometry owing to effective metal to olefin π back bonding in this geometry.^{2d,e} As complexes **2** are

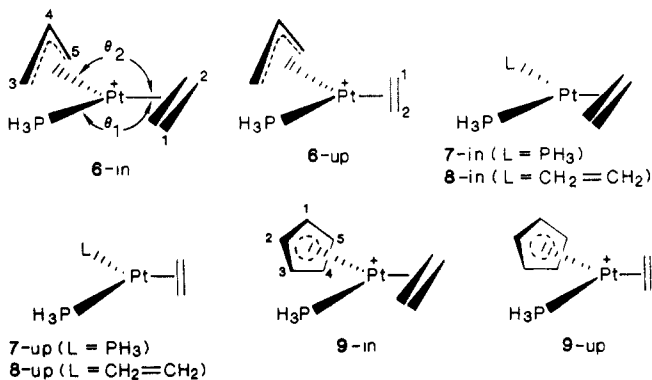


formally derived from **5b** by replacing L (=olefin) with the allyl cation whose HOMO and LUMO are similar to those (π and π^*) of olefins, respectively, one might anticipate that there is a strong electronic demand for the in-plane olefin orientation in **2** as well. We suspect, however, that this is not the case, for the π -accepting ability of the allyl cation is much greater than that of the olefin

ligand in **5b**. The greater electron flow from Pt to the allyl group leaves less electron density on Pt, which in turn decreases the π back bonding ability of Pt with olefin. In fact, the relevant physical properties for assessing the weaker Pt-olefin bond strength of **2** than of **5** are available.²² Notice, also, a contrast between the extensive rotational distortion of the *E*-olefins in **2d** and **2e** and the retention of the in-plane geometry in $\text{Pt}((E)\text{-}p,p\text{-dinitrosilbene})(\text{PPh}_3)_2$.^{11b}

In order to understand the electronic details of the Pt-olefin bond and to find an origin of the flexible olefin coordination mode in **2**, we have examined the electronic structure of $[\text{Pt}(\eta^3\text{-CH}_2\text{CHCH}_2)(\text{CH}_2=\text{CH}_2)(\text{PH}_3)]^+$ (**6**) which serves as a model for **2a-f**, based on the extended Hückel method. The MO calculations were performed for the two limiting olefin conformations: in-plane (**6-in**) and upright (**6-up**). For each conformer, the geometry was roughly optimized by varying the P-Pt-CET angle (θ_1) and the CET-Pt-CAL angle (θ_2), while all the Pt-ligand distances were kept unchanged.²⁴

The computed total energies of **6-in** and **6-up** are nearly the same, the difference being merely 0.07 eV, or 1.6 kcal/mol, in favor of **6-up**.²⁴ For comparison, the analogous calculations on the Pt(0) models, $\text{Pt}(\text{CH}_2=\text{CH}_2)(\text{L})(\text{PH}_3)$ (L = PH_3 (**7**), $\text{CH}_2=\text{CH}_2$ (**8**)),²⁵ showed the distinct preference for the in-plane



geometry by 13 kcal/mol (**7**) or 8 kcal/mol (**8**). These results satisfactorily explain why **2a-f** exhibit a wide range of olefin orientations. They also accord with the failure to freeze the ethylene rotation in **2a** on the NMR time scale down to -100 °C. We suspect, however, that the slightly lower stability of **6-in** than **6-up** is derived from an overestimation of steric factors in **6-in**. The reality may be that the in-plane olefin geometry is electronically preferred in **2a**, **2b**, and **2f**, albeit not very strongly. In this respect, a Mulliken population analysis appears particularly informative. Thus, **6-in** was found to have somewhat larger interatomic Pt-C(ethylene) total overlap populations (Pt-C₁ = 0.246, Pt-C₂ = 0.241) compared with **6-up** (Pt-C₁ = 0.234, Pt-C₂ = 0.231).²⁶ The origin of the electronically favored in-plane conformer is discussed below on the basis of fragment molecular orbital analysis.

The frontier orbitals of the fragment $[\text{Pt}(\eta^3\text{-CH}_2\text{CHCH}_2)(\text{PH}_3)]^+$ and the way they interact with ethylene π and π^* orbitals are shown in Figure 3. Some of the fragment orbitals in Figure 3 have complicated shapes due to a low molecular symmetry. The LUMO (**6a**) of $[\text{Pt}(\eta^3\text{-CH}_2\text{CHCH}_2)(\text{PH}_3)]^+$ can be recognized as an antibonding MO made of the allyl nonbonding and Pt d orbitals largely $d_{x^2-y^2}$ in character, while the occupied **1a** is its

(22) Compare, e.g., the following parameters between **2a** and $\text{Pt}(\text{CH}_2=\text{CH}_2)(\text{duroquinone})(\text{PCy}_3)$:¹³ C=C length (1.33 Å versus 1.398 Å); Pt-C(ethylene) length (2.224 and 2.253 Å versus 2.153 and 2.186 Å); $J[\text{Pt-C}(\text{ethylene})]$ (82 Hz²³ versus 111 Hz).

(23) Kurosawa, H.; Asada, N.; Urabe, A.; Emoto, M. *J. Organomet. Chem.* **1984**, 272, 321.

(24) The calculations were done with the Pt-C(olefin) distances being set as 2.15 Å for the purpose of comparison with related complex models. Elongation of $r(\text{Pt-C})$ in **6** from 2.15 to 2.20 Å, a value close to that in **2a**, resulted in little change of the relative stabilities of **6-in** and **6-up**.

(25) The spectator ethylene ligand (=L) in **8** was kept in-plane coordinated.

(26) The corresponding values for the Pt(0) models are 0.279 (**7-in**) versus 0.210 (**7-up**), or 0.275 and 0.264 (**8-in**) versus 0.226 (**8-up**).

(20) Hine, J. *Structural Effects on Equilibria in Organic Chemistry*; John-Wiley: New York, 1975, p 42.

(21) (a) Cramer, R. J. *Am. Chem. Soc.* **1967**, 89, 4621. (b) Ban, E.; Hughes, R. P.; Powell, J. J. *Organomet. Chem.* **1974**, 69, 455. (c) Henry, P. M. *J. Am. Chem. Soc.* **1966**, 88, 1595. (d) Akermarck, B.; Bäckvall, J. E. *Tetrahedron Lett.* **1975**, 819. (e) Joy, J. R.; Orchin, M. *J. Am. Chem. Soc.* **1959**, 81, 310.

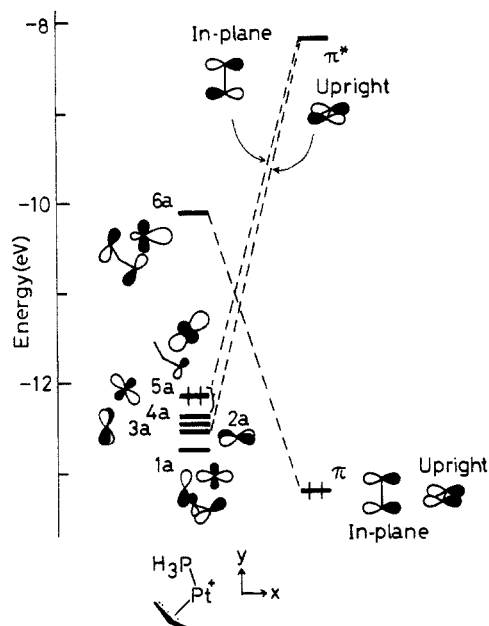


Figure 3. The frontier orbitals of $[\text{Pt}(\eta^3\text{-CH}_2\text{CHCH}_2)(\text{PH}_3)]^+$ and ethylene.

bonding counterpart. The LUMO takes part in the σ interaction with ethylene π for both the **6-in** and **6-up** conformers. With regard to the π interaction, **5a** and **4a** find symmetry match with ethylene π^* in **6-in**,^{27a} whereas in the case of **6-up** a major π contribution comes from **2a**.

According to the fragment analysis, the strength of the Pt-ethylene σ interaction is nearly the same between **6-in** and **6-up**, as is evident in the overlap population between the fragment **6a** and ethylene π orbitals. This was calculated to be 0.230 for **6-in** and 0.226 for **6-up**. On the other hand, the overlap populations associated with ethylene π^* are notably different in the two geometries (**6-in** > **6-up**). Thus, the sum of $2a\text{-}\pi^*$, $3a\text{-}\pi^*$, $4a\text{-}\pi^*$ and $5a\text{-}\pi^*$ overlap populations amounts to 0.215 for **6-in**, to which the $4a\text{-}\pi^*$ and $5a\text{-}\pi^*$ interactions contribute 0.112 and 0.090, respectively. The sum of the corresponding four overlap populations is 0.155 for **6-up**.

It thus appears that, as far as the Pt-ethylene bonding interaction is concerned, the geometry in **6-in** is preferred to that in **6-up**, the origin of which is traced to the better π back bonding interaction in **6-in**. As a matter of fact, 0.336 electron moves from the parent Pt complex to ethylene π^* in **6-in**, while such an electron flow decreases to 0.250 in **6-up**. The higher positioning of **5a** and **4a** in energy relative to **2a** may be a reason behind the stronger π interaction for **6-in** than **6-up**.²⁷ On the other hand, the **6-up** conformation is sterically less crowded, and the preferred orientation of the olefins observed may have been determined by a delicate balance between the electronic and the steric factors.

Next, the MO trends in **6** are compared with those in the related cationic model $[\text{Pt}(\eta^3\text{-C}_3\text{H}_5)(\text{CH}_2=\text{CH}_2)(\text{PH}_3)]^+$ (**9**) which contains steric demands on the ethylene almost similar to those in **6**.²⁸ The change of only the electronic factor on going from **6** (16-electron) to **9** (18-electron) resulted in the remarkable change in the olefin geometry preference. That is, **9** contains the

upright conformer which is ca. 10 kcal/mol more stable than the in-plane one,^{28b} with the Pt-C(ethylene) overlap populations of **9-up** (0.259) being larger than those of **9-in** (0.243 and 0.246). This result is well in accord with the structural and ¹H NMR spectral observations of $[\text{M}(\eta^5\text{-C}_5\text{H}_5)(\text{olefin})(\text{PPh}_3)]^+$ ($\text{M} = \text{Pd}, \text{Pt}$).^{17,23} The higher lying $d\pi$ orbital for π back bonding with the upright ethylene than that with the in-plane ethylene in the fragment $[\text{Pt}(\eta^3\text{-C}_3\text{H}_5)(\text{PH}_3)]^+$, as was pointed out before for isoelectronic fragments, $\text{M}(\eta^5\text{-C}_5\text{H}_5)(\text{PH}_3)$ ($\text{M} = \text{Co}, \text{Ir}$),²⁹ can explain the calculational results of **9**.

Finally, we compare the nature of the Pt-olefin bond in **6** with those in Zeise's salt and its analogues. The occupied frontier orbital levels^{2d} of $[\text{PtCl}_3]^-$ are in principle similar to those of $[\text{Pt}(\eta^3\text{-CH}_2\text{CHCH}_2)(\text{PH}_3)]^+$ in Figure 3. This would result in a comparable electronic requirement for orientation preference of olefins if other factors (e.g., steric) are comparable. However, the LUMO (**6a**) in Figure 3 contains less metal d character than that of $[\text{PtCl}_3]^-$, since in **6a** the metal orbitals are strongly mixed with the allyl nonbonding MO. In addition, **6a** is higher in energy than LUMO of $[\text{PtCl}_3]^-$ (by ca. 0.8 eV). Thus, the Pt-olefin bond in **6** is to be weaker than that in Zeise's salt due to a smaller σ interaction. As a matter of fact, the Pt-C(ethylene) bond lengths in **2a** are considerably longer than those of Zeise's salt and its analogues.^{10,14}

Conclusions

The present structural and MO studies have revealed that complexes **2** are very unique in terms of structures, stabilities, and bonding when compared to the traditional Pt-olefin complexes ranging from **5** to the Zeise's salt class. The Pt-olefin bond strength in **2** is rather weak, in comparison to those in the known Pt-olefin complexes. The requirement of **2** for the in-plane C=C bond orientation is as favorable as that of **5** on the steric basis, but much less so on the electronic basis. Accordingly, the coordination geometry of the bulkier olefin complexes of **2** is dominated by the steric factor, as in the case of Zeise's salt.

Experimental Section

Preparation of Complexes. The following new complexes were prepared in a manner similar to those^{6,23} for analogous complexes **2a**, **2b**, and **2e**. $[\text{Pt}(\text{C}_4\text{H}_7)(\text{CH}_2=\text{CHC}_6\text{H}_4\text{Cl-}o)(\text{PPh}_3)]\text{PF}_6$ (**2c**), colorless needles, mp 153–155 °C dec; Anal. ($\text{C}_{30}\text{H}_{29}\text{F}_6\text{P}_2\text{ClPt}$) C, H. $[\text{Pt}(\text{C}_4\text{H}_7)((E)\text{-MeCH=CHPh})(\text{PPh}_3)]\text{PF}_6\text{-C}_6\text{H}_6$ (**2d**), colorless needles, mp 117–120 °C dec, recrystallized from $\text{CH}_2\text{Cl}_2/\text{benzene}/n\text{-hexane}$; Anal. ($\text{C}_{37}\text{H}_{38}\text{F}_6\text{P}_2\text{Pt}$) C, H. $[\text{Pt}(\text{C}_4\text{H}_7)((Z)\text{-MeCH=CHMe})(\text{PPh}_3)]\text{PF}_6$ (**2f**), colorless needles, mp 138–143 °C dec; Anal. ($\text{C}_{26}\text{H}_{30}\text{F}_6\text{P}_2\text{Pt}$) C, H. $[\text{Pt}(\text{C}_4\text{H}_7)(\text{CH}_2=\text{CHC}_6\text{H}_4\text{Me-}o)(\text{PPh}_3)]\text{PF}_6$, colorless microcrystals, mp 154–156 °C dec; Anal. ($\text{C}_{31}\text{H}_{32}\text{F}_6\text{P}_2\text{Pt}$) C, H. $[\text{Pt}(\text{C}_4\text{H}_7)((E)\text{-MeCH=CHEt})(\text{PPh}_3)]\text{PF}_6$, pale-yellow powders, mp 125–130 °C dec; Anal. ($\text{C}_{27}\text{H}_{32}\text{F}_6\text{P}_2\text{Pt}$) C, H. $[\text{Pt}(\text{C}_4\text{H}_7)((Z)\text{-MeCH=CHEt})(\text{PPh}_3)]\text{PF}_6$, pale-yellow powders, mp 113–115 °C dec; Anal. C, H. The presence of solvent of crystallization in the above complexes, if any, was also confirmed by ¹H NMR spectroscopy. The ¹H NMR spectral data of these complexes are shown in Table S1.

Attempts to isolate an analytically pure sample of $[\text{Pt}(\text{C}_4\text{H}_7)((Z)\text{-MeCH=CHPh})(\text{PPh}_3)]\text{PF}_6$ were unsuccessful, but its formation in solution was confirmed by the ¹H NMR spectrum (Table S1) of a mixture obtained by adding a CD_2Cl_2 solution (0.7 mL) of $\text{Pt}(\text{C}_4\text{H}_7)(\text{Cl})(\text{PPh}_3)$ (70 mg; 0.13 mmol) and $(Z)\text{-MeCH=CHPh}$ (0.03 mL) to a solid sample of AgPF_6 (32 mg; 0.13 mmol), followed by filtration of AgCl .

Stability Measurements. Relative stabilities of substituted styrene and *E*- and *Z*-olefin complexes were determined by ¹H NMR spectroscopy. The methods of sample preparation and instrumental manipulation were the same as those^{6,17,19,23} already described previously. The *K* values thus determined are summarized in Tables III and IV.

Crystal Data and Intensity Data Collection. All the crystals of **2a-f** are colorless prisms. Crystal data are summarized in Table V. The accurate unit-cell dimensions were determined by the least-squares fit of 2θ values of 25 reflections.

On a Rigaku automated, four-circle diffractometer were mounted well-shaped crystals with the following approximate dimensions: 0.20 ×

(27) (a) Both **4a** and **5a** contain comparable degrees of d_{xy} and d_{z^2} contributions. (b) As discussed before,^{24c} the larger separation of the two $d\pi$ orbitals (for the π interaction with the in-plane and the upright ethylene) in **7** and **8** (0.8–1 eV) than in **6** leads to the stronger in-plane preference in **7** and **8**.

(28) (a) The steric congestions about the ethylene in the optimized in-plane geometries of **6-in** and **9-in** are almost the same. (b) We also calculated energies of a model which was constructed by adding two hydrogens to C^3 and C^4 of the C_3H_5 ring of **9** from the backside with respect to Pt and in the perpendicular direction to the C_3H_5 ring, so that the C_3 ring exerts the same steric effect as in **9** but binds to Pt in a η^3 -fashion ($\text{C}^1, \text{C}^2, \text{C}^5$). In this hypothetical model the upright conformer was only less than 1 kcal/mol more stable than the in-plane one.

(29) (a) The upright $d\pi$ orbital (HOMO), which is more than 1 eV higher in energy than the in-plane $d\pi$ orbital, is directed somewhat away from the metal-olefin axis toward PH_3 .^{29b,c} (b) Hoffmann, P.; Padmanabhan, M. *Organometallics* **1983**, *2*, 1273. (c) Silvestre, J.; Calhorda, M. J.; Hoffmann, R.; Stoutland, P. O.; Bergman, R. G. *Ibid.* **1986**, *5*, 1841.

Table V. Crystal Data

	2a	2b	2c	2d	2e	2f
olefin	ethylene	styrene	<i>o</i> -chlorostyrene	(<i>E</i>)- β -methylstyrene	(<i>E</i>)-2-butene	(<i>Z</i>)-2-butene
formula	C ₂₄ H ₂₆ Pt,PF ₆	C ₃₀ H ₃₀ Pt,PF ₆	C ₃₀ H ₂₉ ClPt,PF ₆ 0.5CH ₂ Cl ₂	C ₃₁ H ₃₂ Pt,PF ₆ C ₆ H ₆	C ₂₆ H ₃₀ Pt,PF ₆	C ₂₆ H ₃₀ Pt,PF ₆
formula wt	685.5	761.6	838.5	853.7	713.6	713.6
<i>F</i> (000)	1328	1488	3272	1688	1392	1392
cryst system	monoclinic	monoclinic	orthorhombic	monoclinic	monoclinic	monoclinic
space group	<i>P</i> 2 ₁ / <i>n</i>	<i>P</i> 2 ₁ / <i>n</i>	<i>Pccn</i>	<i>P</i> 2 ₁ / <i>c</i>	<i>P</i> 2 ₁ / <i>c</i>	<i>P</i> 2 ₁ / <i>c</i>
<i>a</i> (Å)	9.610 (2)	15.560 (3)	11.421 (2)	11.408 (2)	13.886 (2)	11.149 (2)
<i>b</i> (Å)	10.786 (4)	11.342 (3)	27.127 (6)	14.910 (10)	11.872 (4)	15.460 (3)
<i>c</i> (Å)	24.082 (8)	17.594 (3)	20.414 (4)	21.397 (3)	16.740 (2)	15.701 (2)
β (°)	91.77 (3)	110.91 (3)		103.17 (2)	91.17 (1)	90.21 (2)
<i>V</i> (Å ³)	2495.0 (14)	2900.6 (9)	6325.0 (21)	3543.8 (23)	2759.2 (9)	2706.2 (7)
<i>D</i> _c (g cm ⁻³)	1.825	1.744	1.761	1.600	1.718	1.751
<i>Z</i>	4	4	8	4	4	4
μ (Mo K α) (mm ⁻¹)	6.10	5.26	5.00	4.32	5.52	5.63

Table VI. Refinement Conditions

	2a	2b	2c	2d	2e	2f
no. of reflns used ($ F_o \geq 3\sigma(F_o)$)	3574	4918	4253	5735	4814	4064
final <i>R</i> value	0.070	0.049	0.084	0.059	0.068	0.069
final <i>R</i> _w value	0.090	0.060	0.114	0.065	0.086	0.089
parameters in weighting scheme (see text)						
<i>a</i>	0.0283	0.0026	-0.0277	-0.0251	-0.0144	-0.0100
<i>b</i>	-0.0001	0.0011	0.0067	0.0046	0.0055	0.0045

Table VII. Extended Hückel Parameters

	orbital	<i>H</i> _{ii} , eV	exponent ^a
Pt	5d	-12.59	6.013 (0.6334) + 2.696 (0.5513)
	6s	-9.077	2.554
	6p	-5.475	2.554
P	3s	-18.6	1.60
	3p	-14.0	1.60
C	2s	-21.4	1.625
	2p	-11.4	1.625
H	1s	-13.6	1.3

^aThe d function is a double- ζ type.

0.30 × 0.35, 0.25 × 0.30 × 0.40, 0.25 × 0.35 × 0.35, 0.15 × 0.30 × 0.35, 0.25 × 0.30 × 0.30, and 0.30 × 0.25 × 0.20 mm for 2a–f, respectively. The quality of each crystal was established by diffraction profiles examined by the ω -scan of several strong reflections. Integrated intensities were collected by the θ -2 θ scan technique with Mo K α radiation ($\lambda = 0.71069$ Å) with graphite-monochromator (for 2a–d) or Zr-filter (for 2e–f). The scan speed was 4 deg min⁻¹ in 2 θ and the scan width was $\Delta 2\theta = (2.0 + 0.70 \tan \theta)^\circ$. Background intensities were measured for 5 s at each end of a scan. Three or four standard reflections measured at regular intervals to monitor the stability and orientation of the crystals showed no significant decay throughout the data collection. Totals of 5448, 6342, 6917, 7718, 6025, and 5908 independent reflections were collected within 2 θ up to 54° ($\sin \theta/\lambda = 0.639$ Å⁻¹) for 2a–f, respectively. Corrections for Lorentz and polarization effects were applied to the intensity data. No absorption corrections were carried out in view of the small size and uniform shape of the crystals, which might limit the accuracy of the present structure determinations.

Structure Solution and Refinement. All the structures except for 2b were solved by the heavy-atom method. The structure of 2b was established by using that of [Pd(η^3 -C₅H₅)(styrene)(PPh₃)]PF₆.⁵ All the non-hydrogen atoms were reasonably found on the Fourier maps that were based on the position of the Pt atom determined from the Patterson function. On the Fourier maps, the solvent molecules CH₂Cl₂ and C₆H₆ were also located for 2c and 2d, respectively. The structures were refined by the block-diagonal least-squares procedure (HBL5-V),³⁰ the function minimized being $\sum w(|F_o| - |F_c|)^2$. On the difference Fourier maps after anisotropic refinement, electron densities assigned to all the hydrogen atoms were found at essentially the same positions calculated by stereochemical considerations, which were included in further refinement. The weighting scheme used is $w = (\sigma_{cs}^2 + a|F_o| + b|F_c|^2)^{-1}$, where σ_{cs} is the standard deviation obtained from the counting statistics, and *a* and *b* are constants adjusted during the refinement cycles. Table VI summarizes the conditions for the course of refinements including the final *R* and *R*_w

values, where $R = \sum ||F_o| - |F_c|| / \sum |F_o|$ and $R_w = \{\sum w(|F_o| - |F_c|)^2 / \sum w|F_o|^2\}^{1/2}$. The atomic scattering factors for non-hydrogen atoms were taken from the *International Tables for X-ray Crystallography*³¹ and those for hydrogen atoms from Stewart et al.³² The final atomic positional parameters, together with the *B*_{eq} values,³³ are listed in Table S5. Tables of anisotropic temperature factors for non-hydrogen atoms, atomic parameters for hydrogen atoms, and observed and calculated structure factors are available as supplementary material (Tables S6–S8).

All the computations were carried out on ACOS 900 and ACOS 850 computers at the Crystallographic Research Center, Institute for Protein Research, Osaka University.

Acknowledgment. The authors thank Dr. H. Kageyama and K. Murakawa for their help in X-ray experiments and valuable discussions. Partial support of this work by a Grant-in-aid for Scientific Research, Ministry of Education, Japan (62215021), is gratefully acknowledged.

Appendix

The parameters of the extended Hückel calculations³⁴ are listed in Table VII. A weighted *H*_{*ij*} formula was used for calculations. Geometrical assumptions included the following: η^3 -allyl, Pt–C³ = Pt–C⁵ = 2.21 Å, Pt–C⁴ = 2.17 Å, C³–C⁴ = C⁴–C⁵ = 1.40 Å, C–H = 1.08 Å, C³–C⁴–C⁵ = 120°, the angle between the allyl and the coordination planes is 115°, terminal allyl hydrogens are bent back by 10°; ethylene, Pt–C = 2.15 Å, C–C = 1.40 Å, C–H = 1.08 Å, ethylene hydrogens bent back by 10°; cyclopentadienyl, Pt–C = 2.34 Å, C–C = 1.42 Å, C–H = 1.08 Å, C₅H₅ is planar; PH₃, Pt–P = 2.30 Å (6, 9) or 2.32 Å (7, 8), P–H = 1.42 Å, PH₃ tetrahedral.

The geometrical parameters in the energy minimum of each isomer correspond to the following: $\theta_1 = 105^\circ$ (6-in and 9-in), 100° (6-up and 9-up), 117.5° (8-in), 110° (8-up); $\theta_2 = 130^\circ$ (6-in and 6-up); P–Pt–P = 110° (7-in) and 130° (7-up); CET–Pt–CET 125° (8-in and 8-up); CET–Pt–CCP = 130° (9-in and 9-up) (CCP = center of C₅H₅).

Registry No. 2 (olefin = CH₂=CHC₂H₄Me-*o*), 113509-09-4; 2 (olefin = (*E*)-MeCH=CHEt), 95099-26-6; 2 (olefin = (*Z*)-MeCH=CHEt), 95189-86-9; 2 (olefin = (*Z*)-MeCH=CHPh), 95189-88-1; 2 (olefin =

(31) *International Tables for X-ray Crystallography*; Kynoch Press: Birmingham, 1974; Vol. IV, p 71.

(32) Stewart, R. F.; Davidson, E. R.; Simpson, W. T. *J. Chem. Phys.* **1965**, *42*, 3175.

(33) Hamilton, W. C. *Acta Crystallogr.* **1959**, *12*, 609.

(34) (a) Hoffmann, R. *J. Chem. Phys.* **1963**, *39*, 1397. (b) Summerville, R. H.; Hoffmann, R. *J. Am. Chem. Soc.* **1976**, *98*, 7240.

(30) Ashida, T. *The Universal Crystallographic Computing System-Osaka*, 2nd ed., The Computation Center: Osaka University, 1979; p 53.

CH₂=CHC₆H₄Me-*m*), 113509-11-8; 2 (olefin = CH₂=CHC₆H₄Cl-*m*), 113509-13-0; 2a, 93612-05-6; 2b, 79730-87-3; 2c, 113509-07-2; 2d, 95099-28-8; 2e, 93712-13-1; 2f, 95340-41-3; 3 (X = *m*-Me), 113509-14-1; 3 (X = *m*-Cl), 113509-15-2; 4 (X = *o*-Me), 113533-04-3; 4 (X = *o*-Cl), 113509-16-3; 6, 113509-17-4; 7, 31941-73-8; 8, 113509-18-5; 9, 113509-19-6; Pt(C₄H₇)(Cl)(PPh₃), 35770-10-6.

Supplementary Material Available: ¹H NMR data for new

complexes (Table S1), bond lengths (Table S2), bond angles (Table S3), equations of least-squares planes (Table S4), final atomic positional parameters (Table S5), anisotropic temperature factors (Table S6), and atomic parameters (Table S7) (29 pages); listing of observed and calculated structure factors (Table S8) (73 pages). Ordering information is given on any current masthead page.

Host-Guest Interactions: A Fluorescence Investigation of the Solubilization of Diphenylpolyene Solute Molecules in Lipid Bilayers

Mary T. Allen, Laerte Miola, and David G. Whitten*

Contribution from the Department of Chemistry, University of Rochester, Rochester, New York 14627. Received August 19, 1987

Abstract: The photophysics of the chromophores 1,4-diphenyl-1,3-butadiene (DPB), 1,6-diphenyl-1,3,5-hexatriene (DPH), and their corresponding 4,4'-dialkyl-substituted derivative molecules, 4B4A and 4H4A, show large concentration effects in the ordered "gel" or "crystalline" phase below the phase transition temperature, T_c , of phospholipid vesicles. The phosphatidylcholine probe DPHpPC shows a similar dependence of its fluorescence intensity on concentration. The solubility of guest-impurity molecules in lipid bilayers is discussed in terms of possible conformational distortion of the chromophores and phase separation of solute within the bilayer, creating local "defect" sites in which the morphology of the bilayer is changed. Measurements of the steady-state anisotropy of these molecules do *not* reflect unusual solute/lipid interactions. Large limiting values of 0.28-0.30 were obtained for the anisotropy of both DPH and 4H4A at temperatures below T_c . At high temperatures above T_c , DPH experiences nearly isotropic rotation ($r = 0.06$) while that of 4H4A continues to be hindered ($r = 0.14-0.16$) in DPPC and DSPC vesicles. Fluorescence depolarization studies of DPB and 4B4A indicate that the fluidity of bilayer interiors decreases with vesicles formed from phospholipids of increasing chain length in the series DMPC, DPPC, and DSPC.

From a photophysical standpoint, *trans,trans,trans*-1,6-diphenyl-1,3,5-hexatriene (DPH) is scarcely the prototype polyene. Yet, DPH fluorescence is intense, relatively long-lived, and sensitive to its environment. At the same time, DPH is assumed to be relatively compatible with membranes due to its nonpolar hydrocarbon structure. These features and the long rodlike structure of DPH, similar to fatty acids and to the visual pigment *trans*-retinal, have prompted its wide use as a probe of membrane structure and dynamics. The fluorescence quantum yield, lifetime, and depolarization of the DPH chromophore are often suggested as parameters that may be measured and interpreted in terms of the physical characteristics of lipid bilayers.¹⁻⁶ However, there remains a controversy as to the specific details of its photophysics as well as the precise location of DPH in bilayers.⁷⁻¹² Critical to the use of DPH as a sampler of the bilayer microenvironment is confidence that it is solubilized in the hydrocarbon interior without causing significant perturbation.

This paper presents results obtained from steady-state ab-

sorption and fluorescence studies of DPH and 1,4-diphenyl-1,3-butadiene (DPB) and their surfactant derivatives 4H4A and 4B4A, respectively (see Chart I), when incorporated into phospholipid vesicles. In addition to these compounds we have also investigated the behavior of 2-(3-(diphenylhexatrienyl)propanoyl)-3-palmitoyl-L- α -phosphatidylcholine (DPHpPC), a DPH-containing phosphatidylcholine. We find that the fluorescence properties of these diphenylpolyene molecules in synthetic membranes are quite complex and show sensitivity to the relative concentrations of solute and lipid as well as to the phase of the bilayer. Although emission from these chromophores can be interpreted in terms of what is known about their solution photophysics, our results emphasize the dynamic nature of solute/lipid interactions and the caution with which any "probe" study must be approached.

To better understand the behavior of polyene chromophores, it is useful to review the salient features of the photophysics of the shortest member of the diphenylpolyene series, *trans*-stilbene (TS). It has been established that the excited singlet state behavior of TS is dominated by two processes.¹³ Fluorescence decay from the first excited singlet state (of B_u symmetry) competes effectively with the activated twisting of the molecule into a perpendicular geometry (see Figure 1). This perpendicular excited state decays to an energy maximum on the ground-state potential surface from which either the *cis* or *trans* isomer is produced. There is a small energy barrier of 3.5 kcal/mol for forming the twisted "p" excited state.¹⁴ This energy barrier is attributed to an avoided crossing of the ¹B_u* surface with a second excited ¹A_g* state as the molecule rotates out of its planar conformation. The height of the barrier to photoisomerization is a function of both the solvent polarity

- (1) Shinitsky, M.; Barenholz, Y. *Biochim. Biophys. Acta* **1978**, *515*, 367.
- (2) Pottel, H.; Van der Meer, W.; Heereman, W. *Biochim. Biophys. Acta* **1983**, *730*, 181.
- (3) Chen, L. A.; Dale, R. E.; Roth, S.; Brand, L. *J. Biol. Chem.* **1977**, *252*, 2163.
- (4) Lakowicz, J. R.; Prendergast, F. G.; Hogan, D. *Biochemistry* **1979**, *18*, 508.
- (5) London, E.; Feigenson, G. W. *Biochim. Biophys. Acta* **1981**, *649*, 89.
- (6) Cranney, M.; Cundall, R. B.; Jones, G. R.; Richards, J. T.; Thomas, E. W. *Biochim. Biophys. Acta* **1983**, *735*, 418.
- (7) Cundall, R. B.; Johnson, J.; Jones, M. W.; Thomas, E. W.; Munro, I. H. *Chem. Phys. Lett.* **1979**, *64*, 39.
- (8) Baretz, B. H.; Singh, A. K.; Liu, R. S. *Nouv. J. Chim.* **1981**, *5*, 297.
- (9) Gerner, H. J. *Photochem.* **1982**, *19*, 343.
- (10) Andrich, M. P.; Vanderkooi, J. M. *Biochemistry* **1976**, *15*, 1257.
- (11) Davenport, L.; Dale, R. E.; Bisby, R. H.; Cundall, R. B. *Biochemistry* **1985**, *24*, 4097.
- (12) Davenport, L.; Knutson, J. R.; Brand, L. *Biochemistry* **1986**, *25*, 1811.

- (13) Saltiel, J., et al. *Org. Photochem.* **1973**, *3*, 1.
- (14) Saltiel, J.; Charlton, J. L. In *Rearrangements in Ground and Excited States*; de Mayo, P., Ed.; Academic: New York, 1980; Vol. 3 and references therein.